

# Radiocarbon

1980

## MODELING THE CARBON SYSTEM

WALLACE S BROECKER, TSUNG-HUNG PENG, and  
RICHARD ENGH\*

Lamont-Doherty Geological Observatory  
and the Department of Geological Sciences,  
Columbia University, Palisades, New York 10964

**ABSTRACT.** Claims that forest cutting during the last few decades has contributed significantly to the buildup in atmospheric CO<sub>2</sub> have cast doubt on the validity of models used to estimate CO<sub>2</sub> uptake by the ocean. In this paper we review the existing models and conclude that the box-diffusion model of Oeschger and his co-workers provides an excellent fit to the average distributions of natural and bomb-produced radiocarbon. We also take the first steps toward a more detailed ocean model which takes into account upwelling in the equatorial zone and deep water formation in the polar zone. The model is calibrated using the distribution of bomb-produced and cosmic ray-produced radiocarbon in the ocean. Preliminary calculations indicate that the fossil fuel CO<sub>2</sub> uptake by this model will be greater than that by the box-diffusion model of Oeschger and others (1975) but not great enough to accommodate a significant decline in the mass of the terrestrial biosphere over the past two decades.

### INTRODUCTION

Two problems of interest to this conference require models of the carbon cycles operating at the earth's surface. 1) The prediction of future atmospheric CO<sub>2</sub> levels based on fossil fuel use scenarios. 2) The deconvolution of the  $\Delta^{14}\text{C}$  changes for atmospheric CO<sub>2</sub> (reconstructed from measurements on tree rings of known age) to yield the temporal history of the production rate of radiocarbon.

The purpose of this paper is to review the status of existing models and to propose a strategy through which these models might be improved. In a sense, this paper is an update of the review of carbon cycle models published by Broecker and others (1979).

The secret of successful geochemical modeling is to mimic the important natural processes employing only transport parameters whose values can be reliably estimated. As our ability to pry loose the secrets of nature's kinetics has proven rather limited, the models we use are, by necessity, rather simple.

Figure 1 shows five important earth surface carbon reservoirs normally identified for the purposes of this modeling: 1) the atmosphere, 2) the ocean, 3) the terrestrial biosphere, 4) soils, 5) sediments.

Although the sedimentary reservoir contains the vast majority of the carbon, it does not play a significant role in the models currently in use. The reason is that the rate of transfer of carbon between this "passive" and the other four "active" reservoirs is quite small compared to the

\* Participant in undergraduate Summer Institute on Planets and Climate at NASA/GISS and Columbia University; current address Augustana College, South Dakota

rates of cycling of carbon among the four active reservoirs. With one major exception the assumption is made that the transfer of carbon to and from the sedimentary reservoir is sufficiently small and sufficiently constant that the distribution of carbon between this passive reservoir and the composite of the four "active" reservoirs remains constant during the course of any of the perturbations of interest to modelers. The exception is, of course, the burning of fossil fuels which involves a transfer of sedimentary carbon to the atmosphere.

The current sizes of the atmospheric and oceanic carbon reservoirs are accurately known; that of the living biosphere and of the soil reservoir are known, respectively, to about 25 percent and 50 percent.

The rate of transfer of carbon between the ocean and atmosphere is known to about  $\pm 20$  percent. The rate of transfer between the atmosphere and terrestrial biosphere is known to perhaps  $\pm 50$  percent, while that between soils and the atmosphere is little more than an educated guess.

For most modeling applications the four active reservoirs must be subdivided. In the case of the atmosphere, the stratosphere must sometimes be treated as a separate reservoir. It constitutes about 15 percent of the atmosphere and is ventilated with tropospheric air on the time scale of about five years (Machta, 1972). While for most applications this distinction can be neglected as discussed below, in the case of the bomb  $^{14}\text{C}$  inventory the separation is important. At a minimum the terrestrial biosphere must be divided into at least two sub-reservoirs: wood and

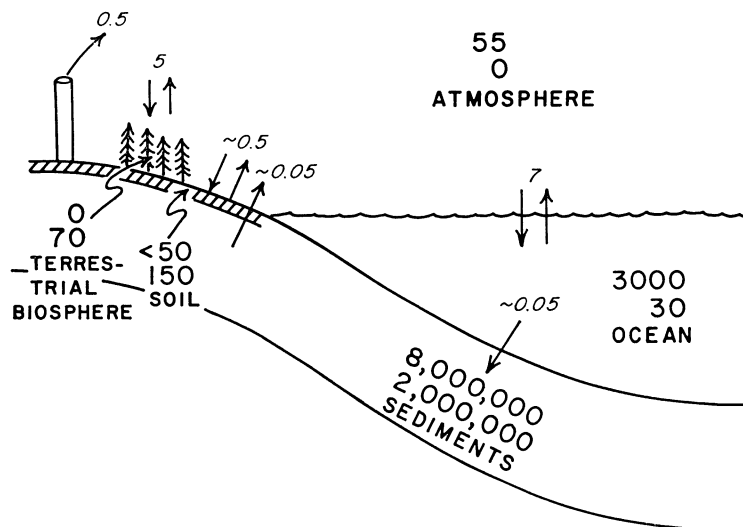


Fig 1. Diagram showing the five major carbon reservoirs named in the text. The amounts of inorganic (upper number) and organic (lower number) carbon in each reservoir are given by the heavy type face numbers (in units of  $10^{15}$  moles). The fluxes between the reservoirs are given by the light type face numbers (the units are  $10^{14}$  moles/year).

other living organic matter (small plants, and tree rootlets, bark and leaves). The former has a long response time ( $\sim 30$  years) and the latter has a short response time ( $< 2$  years). The soil reservoir should also be subdivided. Unfortunately, our knowledge of the replacement time of soil components is too primitive to permit a meaningful division (see Schlesinger, 1977, for a discussion of this problem). Much of the discussion which follows will be devoted to strategies for developing adequate subdivisions of the ocean.

To be acceptable, any model of the carbon system must adequately reproduce the following observations: 1) the distribution of natural radiocarbon, 2) the distribution of fossil fuel  $\text{CO}_2$ , 3) the distribution of bomb-produced  $^{14}\text{C}$ .

As shown below, we have now gathered enough information regarding the distribution of these tracers to make this test a rather demanding one.

The majority of the modeling done to date has been carried out using the three box atmosphere-ocean model of Craig (1957) or the box-diffusion model of Oeschger and others (1975). In the former, the ocean is divided into a well mixed surface and deep layer. In the latter, the well mixed surface layer is coupled to a deep layer through which material is transported by eddy diffusion. Both models employ well mixed atmospheres that interact with the well mixed upper ocean box by gas exchange. In both models the oceanic mixing parameter is chosen to fit the distribution of natural  $^{14}\text{C}$  within the sea (*ie*, the between-box transfer rate in the 3-box model and the vertical diffusivity in the box-diffusion model). In the box-diffusion model the thickness of the surface layer is taken to be that of the actual wind mixed layer (average thickness, 75m). In the three-box model the surface layer has been given thicknesses ranging from 50m up to 500m. The rationale for adopting a thicker layer is that the midpoint between the temperature of surface water and that of deep water at any given place in the ocean ranges from 200 to 600m. While this choice has only minor consequences in the original application of the three-box model (*ie*, establishing the mean ventilation time for the deep sea based on  $^{14}\text{C}$  data) it is important in connection with response of the model to the fossil fuel and solar induced transients.

It is our conclusion that for the applications mentioned above the box-diffusion model is superior to the three-box model. Our reason is that the diffusion model reproduces the general depth distribution observed for bomb-produced tracers within the sea without resorting to an arbitrary thickening of the surface mixed layer. We were also influenced in this decision by the observation that the diffusivity which yields the proper deep water  $^{14}\text{C}$  age in the box-diffusion model also yields the proper mean depth distribution of the bomb-produced tracer  $^3\text{H}$ .

#### *Evaluation of the box-diffusion model*

As stated above, the values of the two free parameters in the Oeschger and others model were chosen to match the distribution of natural radiocarbon (the mixed layer thickness of 75m is selected to match that ob-

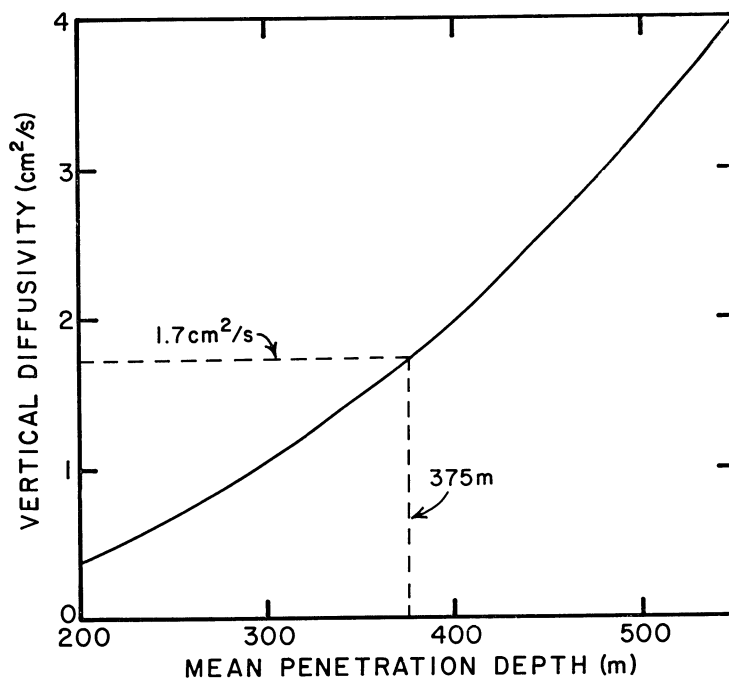


Fig 2. Relationship between vertical diffusivity and mean penetration depth of tritium in 1973 as calculated from the Oeschger and others model. The dashed lines show the mean penetration depth and corresponding diffusivity obtained from the GEOSECS tritium data.

served in the sea). Subsequent work has verified the suitability of the values adopted for these parameters by Oeschger and his co-workers. A recent global survey using the radon method (Peng and others, 1979) yields an estimate of 16 moles/m<sup>2</sup>year for the mean CO<sub>2</sub> invasion rate into the sea. This is somewhat smaller than the value of 21 moles/m<sup>2</sup>year adopted by the Swiss group. The vertical distribution of tritium in the ocean as obtained during the GEOSECS program can be used to make an independent estimate of the diffusivity. As summarized in tables 1 and 2, the mean penetration depth of tritium (as of 1973) was about 375m. Figure 2 shows the relationship between mean penetration depth and diffusivity for an Oeschger-type model (tritium is added to the surface ocean using the atmospheric delivery time history proposed by Weiss, Roether, and Dreisigacker, 1978). The value obtained in this way is 1.7cm<sup>2</sup>/sec as opposed to the 1.25cm<sup>2</sup>/sec value adopted by the Swiss group.<sup>1</sup>

<sup>1</sup>We do not mean to imply that the process of vertical eddy mixing actually occurs within the body of the main oceanic thermocline. Indeed, the values we require are an order of magnitude greater than those permitted by conventional oceanographic wisdom (see Garrett, 1979, for summary). The vertical eddy coefficients used here should rather be thought of as parameters that take into account all the processes that transfer tracers across density horizons. In addition to vertical mixing by eddies, these include mixing induced by sediment friction at the ocean margins and mixing along the surface in the regions where density horizons outcrop.

TABLE I

For each GEOSECS station at which tritium measurements were made the mean penetration depth of tritium was obtained by dividing the total water column tritium inventory (in units of TU-meters) by the mean mixed layer tritium content (mean of all measurements at depths less than 75m). The penetration depths marked with an asterisk are for stations at which there is a sub-surface tritium maximum. The tritium measurements were made at the University of Miami (Ostlund, Dorsey, and Brescher, 1976; Ostlund and others, 1978).

Sta no.	Lat	Long	Surf <sup>3</sup> H TU	Inventory TU-M	Mean depth M
Atlantic >45°N					
17	74.9°N	1.1°W	5.1	6200	1220
18	70.0°N	0.0°	7.3	7700	1050
19	64.2°N	5.6°W	7.2	5980	830
11	63.5°N	35.2°W	6.6	8700	1320
23	60.4°N	18.6°W	7.5	7500	1000
5	56.9°N	42.6°W	7.8	8700	1110
3	51.0°N	43.1°W	12.1	11,300	930
					Mean 1060
Atlantic 45°N-15°N					
27	42.0°N	42.0°W	8.5	7900	930
29	36.0°N	47.0°W	7.3	6300	660
121	36.0°N	68.0°W	5.9	5000	850
120	33.3°N	56.5°W	6.5	4700	720
30	31.8°N	50.8°W	6.8	5100	750
117	30.7°N	39.0°W	7.1	5000	710
115	28.0°N	26.0°W	7.2	4000	560
31	27.0°N	53.5°W	7.7	5100	660
32	23.8°N	54.0°W	5.5	3300	600
33	21.0°N	54.0°W	5.0	3300	670
34	18.0°N	54.0°W	4.5	2800	630*
					Mean 700
Atlantic 15°N-15°S					
37	12.0°N	51.0°W	4.0	1400	360
40	3.9°N	38.5°W	2.5	460	190
48	4.0°S	39.0°W	2.2	380	170
49	7.9°S	28.2°W	2.2	390	180
54	15.0°S	28.2°W	2.2	500	220
					Mean 220
Atlantic 15°S-45°S					
56	21.0°S	33.0°W	2.2	720	330
58	27.0°S	37.0°W	2.2	690	310
60	33.0°S	42.5°W	2.2	770	350
64	39.0°S	48.5°W	1.6	520	320
93	41.8°S	18.5°W	1.6	510	310
67	45.0°S	51.0°W	1.35	540	400
					Mean 340
Atlantic >45°S					
68	48.6°S	46.0°W	0.81	360	440
91	49.6°S	11.5°E	0.91	280	310
74	55.0°S	50.1°W	0.76	230	300

TABLE 1 (continued)

Sta no.	Lat	Long	Surf <sup>3</sup> H TU	Inventory TU-M	Mean depth M
82	56.3°S	24.9°W	0.85	180	210
76	57.7°S	66.1°W	0.98	300	310
77	59.7°S	64.5°W	0.90	200	220
89	60.0°S	0.0°	0.87	120	140
78	61.0°S	63.0°W	0.85	210	250
					Mean 270
Pacific >45°N					
219	53.1°N	177.3°W	7.4	2400	320
218	50.4°N	176.6°W	10.1	2800	280
221	45.2°N	169.4°E	9.4	3100	330
					Mean 310
Pacific 45°N-15°N					
217	44.6°N	177.0°W	9.2	3400	370
216	40.8°N	177.0°W	7.0	3600	510
222	40.2°N	160.5°E	7.4	3500	470
201	34.2°N	127.9°W	14.2	3400	240
202	33.1°N	139.6°W	10.0	3900	390
204	31.4°N	150.0°W	7.9	3600	450
212	30.0°N	159.8°W	7.2	3500	490
213	31.0°N	168.5°W	6.8	3600	530
214	32.0°N	177.0°W	6.7	3700	550
215	37.5°N	177.3°W	6.6	4300	650
223	35.0°N	151.8°E	6.1	5000	820
224	34.2°N	142.0°E	6.1	4700	770
225	32.6°N	161.9°E	6.6	4800	730
226	30.6°N	170.6°E	6.6	4000	610
347	28.5°N	121.5°W	12.5	2500	200
346	25.5°N	121.8°W	13.0	3300	250
227	25.0°N	170.1°E	6.0	3700	610*
345	22.5°N	122.2°W	13.4	2700	200
228	19.0°N	169.4°E	5.4	2800	520*
235	16.8°N	161.4°W	4.7	2300	500*
					Mean 490
Pacific 15°N-15°S					
342	14.5°N	123.1°W	4.0	1000	250*
231	14.1°N	178.5°E	4.8	1950	410*
229	12.9°N	173.5°E	4.1	1800	440*
237	12.5°N	165.4°W	5.6	1350	240*
340	10.5°N	123.6°W	3.5	275	80
238	8.2°N	167.1°W	3.4	1100	330*
239	5.9°N	172.0°W	3.5	950	270
337	4.8°N	124.1°W	2.9	550	190
241	4.5°N	179.0°E	3.2	875	270
336	3.0°N	124.4°W	2.8	400	150
335	1.5°N	124.5°W	2.9	450	160
244	1.0°N	178.9°E	3.2	850	270
246	0.0°	179.0°E	2.9	575	230
334	0.0°	124.6°W	3.1	650	210*
248	1.0°S	179.0°E	2.3	550	240
333	1.5°S	124.6°W	2.4	325	130
332	3.0°S	124.6°W	2.2	250	120
331	4.6°S	125.1°W	2.0	275	140
251	4.6°S	179.0°E	2.4	525	220
330	6.1°S	125.3°W	1.7	200	120
328	9.3°S	125.5°W	1.5	300	200
257	10.2°S	170.0°W	2.2	525	240

TABLE 1 (continued)

Sta no.	Lat	Long	Surf <sup>a</sup> H TU	Inventory TU-M	Mean depth M
327	11.6°S	125.9°W	1.8	400	220
326	14.0°S	126.2°W	1.6	425	270
325	14.6°S	130.9°W	~1.8	450	250
				Mean	225
Pacific 15°S-45°S					
263	16.7°S	167.1°W	2.3	550	240
316	18.8°S	126.6°W	1.65	550	330
324	23.0°S	146.1°W	1.9	650	340
317	23.6°S	127.2°W	1.8	725	400
269	24.0°S	174.5°W	1.9	700	370
310	27.0°S	157.1°W	2.0	700	350
319	28.5°S	127.8°W	1.9	500	260
306	32.8°S	163.6°W	1.9	500	260
320	33.3°S	128.6°W	1.85	525	280
278	36.5°S	179.6°W	1.6	650	410
303	38.4°S	170.1°W	1.45	550	380
321	38.6°S	129.4°W	1.6	400	260
322	43.0°S	129.9°W	1.0	475	475
296	45.0°S	166.6°W	1.3	550	420
				Mean	340
Pacific >45°S					
294	50.6°S	180.0°	0.90	425	470
293	52.7°S	178.1°W	1.00	675	675
291	56.0°S	175.6°W	0.75	550	730
280	56.0°S	170.0°E	0.95	425	450
282	57.6°S	169.6°E	0.90	375	420
290	58.0°S	174.0°W	0.80	310	390
285	61.5°S	170.0°E	0.90	165	180
				Mean	475

TABLE 2

Summary of the mean tritium penetration depths as of 1973 for various parts of the ocean. The numbers in the right hand column are the product of the mean penetration for a given zone times the fraction of ocean area covered by the zone. The penetration depths for the Indian Ocean are taken to be the averages for the Atlantic and Pacific.

	Atlantic m	Pacific m	Global mean m	Fraction ocean area	Contribution to global mean depth m
Antarctic (>45°S)	270	475	375	.169	62
South temperate (45°S-15°S)	340	340	340	.264	90
Equator (15°S-15°N)	220	225	225	.281	63
North temperate (15°N-45°N)	700	490	560	.192	107
North Pacific (>45°N)	—	310	—	.028	9
North Atlantic (>45°N)	1060	—	—	.036	38
Arctic (~>70°N)	—	—	~200	.032	6
Global mean					375

As first shown by Suess (1955), the  $^{14}\text{C}/\text{C}$  ratio in the atmosphere decreased by 2.5 percent between 1850 and 1950 (subsequent measurements lie in the range  $2.3 \pm 0.3$  percent). Suess attributed this decrease to the dilution by  $^{14}\text{C}$ -free fossil-fuel  $\text{CO}_2$ . Stuiver (pers commun) concludes that the tree-ring-based estimate for the fossil fuel effect is a maximum, since part of the observed reduction must be due to a sun-spot-induced reduction in the production rate of  $^{14}\text{C}$ . As the amount of  $\text{CO}_2$  added to the atmosphere as of 1950 was about 10 percent of the  $\text{CO}_2$  present in the atmosphere at that time, the effective mass of carbon into which the fossil fuel  $\text{CO}_2$  molecules had been mixed must in 1950 have been about at least four times the mass of atmospheric carbon. Models of the living terrestrial biosphere suggest that it could provide a carbon mixing mass about  $1.0 \pm 0.3$  the atmospheric mass.<sup>2</sup> Thus, the atmospheric and living biospheric carbon reservoirs taken together provide a dilution factor of  $2.0 \pm 0.3$ . The contribution of the soil reservoir to the dilution is likely small as soil organic molecules on the average are replaced very slowly. However, if a substantial fraction ( $\sim 10$  percent) of this reservoir turns over at a high rate (once every few years) a significant contribution ( $\sim 0.3$  atmospheric masses) would be made to the dilution. Unfortunately, we do not have the information required to quantify the dilution by soil.

In any case, it appears that the ocean must contribute at least two atmospheric carbon masses to the dilution pool. The Oeschger and others (1975) ocean model predicts an ocean dilution mass of four times the atmospheric value. Hence, it passes the Suess effect test.

Druffel and Linick (1978) and Druffel (1980) have measured a decline of about  $1.1 \pm 0.2$  percent in the  $^{14}\text{C}/\text{C}$  ratio in surface ocean water over the period 1850 to 1950 (*ie*, the surface ocean Suess effect is about  $0.45 \pm .10$  the atmospheric Suess effect). The Oeschger model predicts, as of 1950, a ratio of surface ocean to atmosphere Suess effect of .36 (this *ratio* is independent of assumptions made in connection with the biosphere and with regard to the contribution of the decrease in  $^{14}\text{C}$  production to the  $^{14}\text{C}$  decline). Again, the agreement is satisfactory.<sup>3</sup>

Bomb tests carried out during the period 1954-1963 produced about  $700 \times 10^{26}$   $^{14}\text{C}$  atoms. Measurements carried out in the troposphere provide good inventories of the bomb  $^{14}\text{C}$  content of this reservoir over the entire period of interest from 1950 to the present. Machta (1972) published inventories of bomb  $^{14}\text{C}$  in the stratosphere for the period 1965 through 1969. The GEOSECS survey provides an ocean inventory as of

<sup>2</sup> The mass of living biospheric carbon has been estimated by Whittacker and Likens (1975) to be 1.25 times the mass of carbon in the atmosphere.

<sup>3</sup> Nozaki and others (1978) made similar measurements on a coral from Bermuda. They give an oceanic Suess effect about three times larger than that found by Druffel and Linick (1978) or by Druffel (1980). However, their coral showed a large decrease in  $\Delta^{14}\text{C}$  from 1800 to 1860 followed by an increase from 1860 to 1900. Such changes are not expected and were not seen in the Florida Straits or the Belize coral. Whatever caused them may well be responsible for giving a false impression of the magnitude of the oceanic Suess effect.



1973. This information provides another series of checks for carbon models.

The first such test is to determine whether the ocean bomb  $^{14}\text{C}$  inventory measured as part of the GEOSECS program is consistent with the model value. To check this, we have done the following. First the Oeschger and others model was run, using the observed atmospheric time history for  $\Delta^{14}\text{C}$  during the "bomb" era (see fig 3). Second, inventories of excess  $^{14}\text{C}$  (over that in 1955) were determined for each GEOSECS station (see table 3). These values were regionally averaged and a global inventory was made. The result of the box diffusion model calculation using a diffusivity of  $1.25\text{cm}^2/\text{sec}$  and a gas exchange rate of 21 moles/ $\text{m}^2\text{yr}$  is  $290 \times 10^{26}$  atoms (for 1973). The observed ocean inventory was, at that time,  $314 \pm 30 \times 10^{26}$  atoms (see table 4).

The second test was to see whether the model yields a mean  $\Delta^{14}\text{C}$  value equal to the mean observed during the GEOSECS program for surface ocean water. As summarized in table 5, the observed average is  $160 \pm 15\%$  higher than that for the pre-bomb era. The box-diffusion model value for 1973 is 195%. The agreement is satisfactory.

The importance of this second test is that it shows the ratio of the air-sea interface resistance to the vertical mixing resistance within the sea to be of the right magnitude. While a wide range of combinations of gas exchange rate and diffusivity could match the observed inventory, this range is greatly narrowed if a match of both the inventory and the surface value is demanded. Figure 4 shows the combination of gas exchange rate and diffusivity which adequately reproduce both the inventory and surface  $\Delta^{14}\text{C}$ . This approach restricts the gas exchange rate to the range 18 to 25 moles/ $\text{m}^2\text{yr}$  and the vertical diffusivity to the range 1.9 to  $3.3\text{cm}^2/\text{sec}$ .

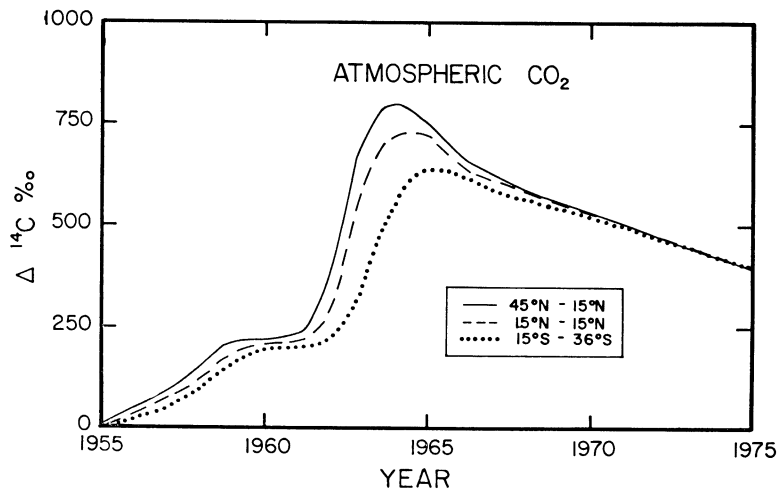


Fig 3. Atmospheric  $\Delta^{14}\text{C}$  as a function of time. The 1962-1975 portions of the curves are based on data by Nydal, Lövseth, and Gulliksen (1979). The early portions of the curves are based on published results by a number of laboratories.

TABLE 3

Excess  $^{14}\text{C}$  inventories for the GEOSECS stations at which  $^{14}\text{C}$  samples were collected. The procedures used to calculate these excesses are described in Peng and Broecker (ms in preparation). The measurements upon which these estimates are based were made by Ostlund at the University of Miami and Stuiver at the University of Washington.

Sta no.	Lat	Long	Total excess $^{14}\text{C}$ 10 <sup>9</sup> atoms/CM <sup>2</sup>
Northern Atlantic (>45°N)			
17	74.9°N	1.1°W	12.4
18	70.0°N	0.0°W	24.0
19	64.2°N	5.6°W	20.2
11	63.5°N	35.2°W	17.1
23	60.4°N	18.6°W	17.5
5	56.9°N	42.6°W	18.6
3	51.0°N	43.1°W	20.6
		Mean	18.6
North Temperate Atlantic (45°N-15°N)			
27	42.0°N	42.0°W	17.9
29	36.0°N	47.0°W	18.4
120	33.3°N	53.5°W	16.4
117	30.7°N	39.0°W	14.8
115	28.0°N	26.0°W	12.1
31	27.0°N	53.5°W	16.9
33	21.0°N	54.0°W	10.5
		Mean	15.3
Equatorial Atlantic (15°N-15°S)			
37	12.0°N	51.0°W	5.2
113	11.0°N	20.5°W	1.6
40	3.9°N	38.5°W	4.4
111	2.0°N	14.0°W	2.5
48	4.0°S	29.0°W	3.3
49	7.9°S	28.2°W	4.4
107	12.0°S	2.0°E	2.0
		Mean	3.3
South Temperate Atlantic (15°S-45°S)			
54	15.1°S	29.5°W	6.4
56	21.0°S	33.0°W	9.0
103	24.0°S	8.5°E	8.7
58	27.0°S	37.0°W	11.0
60	33.0°S	42.5°W	11.6
64	39.1°S	48.5°W	8.3
93	41.8°S	18.5°E	8.7
67	45.0°S	51.1°W	9.4
		Mean	9.1
		Mean (excluding sta 54)	9.5
Antarctic Atlantic (>45°S)			
68	48.6°S	46.0°W	~8
74	55.0°S	50.1°W	~5
82	56.3°S	24.9°W	~3
76	57.7°S	66.1°W	~6
89	60.0°S	0.0°	~2
		Mean	~5

TABLE 3 (continued)

Sta no.	Lat	Long	Total excess <sup>14</sup> C 10 <sup>6</sup> atoms/CM <sup>2</sup>
Northern Pacific (>45°N)			
219	53.1°N	177.3°W	~5
218	50.4°N	176.6°W	~6
		Mean	~6
North Temperate Pacific (45°N-15°N)			
217	44.7°N	177.0°W	9.7
222	40.2°N	160.5°E	9.3
224	34.2°N	142.0°E	22.0
223	35.0°N	151.0°E	21.2
225	32.6°N	161.9°E	20.0
226	30.6°N	170.6°E	15.2
214	32.0°N	177.0°W	14.4
213	31.0°N	168.5°W	13.0
204	31.4°N	150.0°W	11.6
202	33.1°N	139.6°W	10.9
201	34.2°N	127.9°W	8.2
227	25.0°N	170.1°E	14.8
235	16.7°N	161.4°W	9.2
343	16.5°N	123.0°W	4.5
		Mean	13.1
		Mean (excluding stas 235 and 343)	14.2
Equatorial Pacific (15°N-15°S)			
231	14.1°N	178.6°W	9.1
229	12.9°N	173.5°E	8.5
239	5.9°N	172.0°W	5.3
337	4.8°N	124.1°W	4.6
334	0.0	124.6°W	4.2
331	4.6°S	125.1°W	4.4
326	14.0°S	126.2°W	8.3
		Mean	6.3
		Mean (excluding stas 326 and 231)	5.4
South Temperate Pacific (15°S-45°S)			
324	23.0°S	146.1°W	9.9
317	23.6°S	127.2°W	11.0
310	27.0°S	157.1°W	11.6
306	32.8°S	163.6°W	7.3
320	33.3°S	128.6°W	8.3
303	38.4°S	170.1°W	8.4
322	43.0°S	129.9°W	12.3
296	45.0°S	166.7°W	8.7
		Mean	9.7
Antarctic Pacific (>45°S)			
293	52.7°S	175.1°W	~17
282	57.6°S	169.6°E	~11
290	58.0°S	174.0°W	~7
287	69.1°S	173.5°W	~2
		Mean	~9

A final test provided by the bomb  $^{14}\text{C}$  data set is to determine whether the decrease in atmospheric inventory over the period 1965 to 1969 is adequately compensated by ocean plus biosphere uptake. As summarized in table 6, the atmospheric excess  $^{14}\text{C}$  inventory decreased by  $130 \times 10^{26}$  atoms in this four-year period. The Oeschger model predicts an ocean uptake of  $89 \times 10^{26}$  atoms over this same period, leaving  $41 \times 10^{26}$  atoms to be accounted for by uptake by the terrestrial biosphere. If 15 percent of the matter in the terrestrial biosphere is assumed to turn over on a time-scale of less than two years, then the decline in the

TABLE 4  
Summary of the excess  $^{14}\text{C}$  inventories for various regions of the ocean  
(based on data in table 3)

	Atlantic	Pacific	Mean global	Fraction ocean area	Excess $^{14}\text{C}$ $10^{26}$ atoms
	← $10^9$ atoms/ $\text{CM}^2$ →				
Antarctic ( $>45^\circ\text{S}$ )	~5	~9	~7	.167	~40
South temperate ( $45^\circ\text{S}$ - $15^\circ\text{S}$ )	9.5	9.7	9.6	.264	92
Equator ( $15^\circ\text{S}$ - $15^\circ\text{N}$ )	3.3	5.4	5.0	.281	51
North temperate ( $15^\circ\text{N}$ - $45^\circ\text{N}$ )	15.3	14.2	14.6	.192	101
North Pacific ( $>45^\circ\text{N}$ )	—	~6	—	.028	~6
North Atlantic ( $>45^\circ\text{N}$ )	18.6	—	—	.036	19
Arctic Ocean	—	—	~4	.032	~5
					<u><math>314 \pm 35</math></u>

TABLE 5  
Summary of surface bomb  $^{14}\text{C}$  excess (as of 1973)

Region	No. of stas	Measured* $\Delta^{14}\text{C}$ ‰	Prenuclear $\Delta^{14}\text{C}$ ‰	Excess $\Delta^{14}\text{C}$ ‰
ATLANTIC				
North polar	8	50	-70	120
North temperate	8	145	-50	195
Equator	6	85	-65	150
South temperate	6	126	-50	176
Antarctic	6	—	—	~100
PACIFIC				
North polar	4	—	—	~130
North temperate	15	163	-50	213
Equator	5	61	-70	131
South temperate	7	141	-50	191
Antarctic	4	—	—	~115
WHOLE OCEAN				
North polar	(.096)			125
North temperate	(.192)			205
Equator	(.281)			140
South temperate	(.264)			185
Antarctic	(.169)			110
Mean				<u><math>169 \pm 15</math></u>

\* Measured by Stuiver or by Ostlund as part of the GEOSECS program.

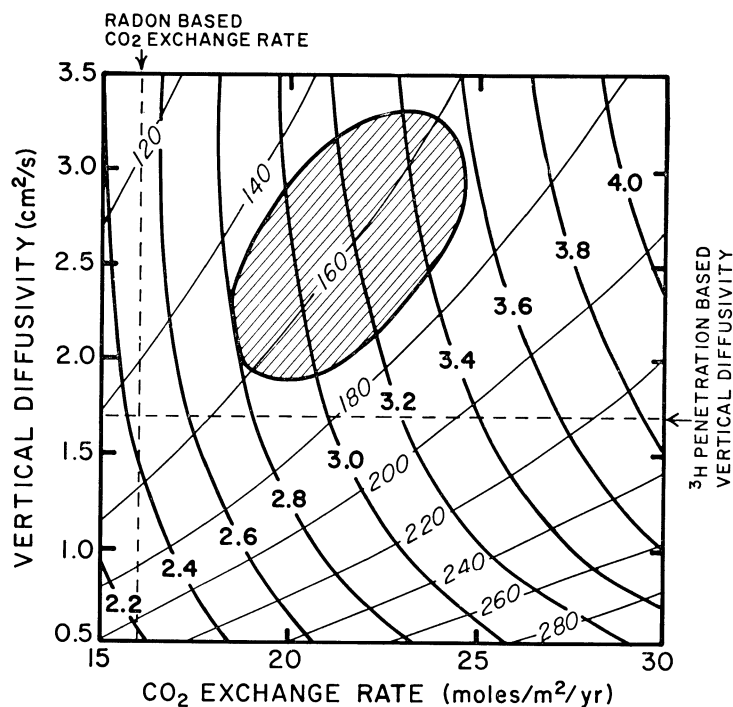


Fig 4. Excess  $\Delta^{14}\text{C}$  for surface water ( $\%$ ) and total bomb  $^{14}\text{C}$  absorbed by the ocean ( $10^{28}$  atoms) as functions of  $\text{CO}_2$  exchange rate and vertical diffusivity. An ellipse is drawn to show the most probable range of surface  $\Delta^{14}\text{C}$  and integrated bomb  $^{14}\text{C}$  of the ocean as of the end of 1973. The corresponding  $\text{CO}_2$  exchange rate is in the range between 19 and 24 moles/m<sup>2</sup>/yr, and the vertical diffusivity is in the range between 1.9 and 3.3 cm<sup>2</sup>/s.

TABLE 6  
Global bomb  $^{14}\text{C}$  inventories for the years 1965 and 1969  
(units  $10^{26}$  atoms)

	1965	1969	1969-1965
Stratosphere*	155	93	-62
Troposphere	267	199	-68
Atmosphere	422	292	-130
Oeschger Ocean**	141	230	+89
Net (terrestrial biosphere)	—	—	-41
Rapid turnover terrestrial biosphere	53	40	-13
Net (wood + soil)	—	—	-54
Wood + soil	—	—	+52
Net ( <i>ie</i> , unaccounted for)	—	—	-2

\* As given by Machta (1972).

\*\* K = 1.25 cm<sup>2</sup>/sec, E = 21 moles/m<sup>2</sup>/yr.

TABLE 7  
Summary of oceanic fossil fuel CO<sub>2</sub> inventories obtained through the use of various sets of parameters for the box-diffusion model\*

	K cm <sup>2</sup> /sec	E moles/m <sup>2</sup> yr	ΣCO <sub>2</sub> 10 <sup>14</sup> moles
Oeschger and others Best case	1.25	21	29.0
Radon based E Tritium based K	1.7	16	31.1
Bomb <sup>14</sup> C Upper limit	3.3	24	42.2
Best fit	2.6	21.5	38.1
Lower limit	1.9	19	33.3
Best estimate this paper	2.2	19	35.1

\* K = vertical diffusivity.  
E = CO<sub>2</sub> exchange rate.

bomb <sup>14</sup>C content of this matter (paralleling that for the troposphere) must have released about  $13 \times 10^{26}$  bomb <sup>14</sup>C atoms. This raises the total to be taken up by the remaining biosphere (wood and soil) to  $54 \times 10^{26}$  atoms. That this uptake is not out of the required range can be seen as follows: wood production averages about  $2.5 \times 10^{15}$  moles of carbon per year (*ie*, half the total photosynthesis). If soil organics are replaced at the rate of one part in 300 per year and if the soil carbon biomass is three times the atmospheric carbon mass, then about  $0.5 \times 10^{15}$  moles of carbon are stored this way each year. Thus, a total of  $3 \times 10^{15}$  moles of carbon is stored each year in the combined wood-soil reservoir. Neglecting the release of bomb <sup>14</sup>C from these reservoirs (it should be small) the net uptake would be  $52 \times 10^{26}$  atoms (*ie*, 96 percent of the unexplained bomb <sup>14</sup>C). Again, the ocean model nicely passes the test.<sup>5</sup>

From the above, it is clear that the parameters used by Oeschger and others might be revised a bit in the light of the radon and bomb tracer data obtained as part of the GEOSECS program. Table 7 compares the fossil fuel CO<sub>2</sub> uptake by the box-diffusion model assuming 1) the Oeschger and others parameters, 2) the GEOSECS radon based gas exchange, and the GEOSECS tritium penetration based diffusivity, 3) the restrictions set by the bomb <sup>14</sup>C data, and 4) our best estimates. These calculations were made using the model calibration atmospheric CO<sub>2</sub> curve described below.

<sup>5</sup> In this calculation we assumed that no man-made production of <sup>14</sup>C occurred during the 1965 to 1969 period. As pointed out by Nydal at this meeting there were Chinese and French tests during this period. Nydal (pers commun) estimates that the tests during this period totaled 17.4 megatons (TNT equivalent) in energy. The total prior to the August 5, 1963 test ban was about 510 megatons. If the <sup>14</sup>C yield (per megaton) of the tests carried out from 1965 to 1969 was the same as that for the tests carried out prior to the test ban, then the amount of bomb <sup>14</sup>C present on the earth was increased by about 3.5 percent during the 1965-1969 period. Inclusion of this production in table 6 would increase the net <sup>14</sup>C unaccounted for from 2 to  $13 \times 10^{26}$  atoms. Nydal's estimates are based on data given by Zander and Araskog (1973) and in the SIPRI Yearbook (1975, 1976).

Because the fossil fuel uptake is rather insensitive to the choice of the  $\text{CO}_2$  exchange rate and depends on the square root of the diffusivity, the range in uptakes is quite small. As of 1973,  $107 \times 10^{14}$  moles of fossil fuel  $\text{CO}_2$  had been produced. If, as suggested by the data of Keeling and his co-workers, 55 percent of this  $\text{CO}_2$  resided in the atmosphere, then  $48 \times 10^{14}$  moles must have resided in the ocean (or in the terrestrial biosphere). None of the values in table 7 exceeds this value.

This observation provides one last test of the Oeschger and others model. Figure 5 shows that the increase in atmospheric  $\text{CO}_2$  content from 1958 to the present is close to half that expected if all the fossil fuel  $\text{CO}_2$  produced accumulated in the air. As the  $\text{CO}_2$  not found in the air must be largely in the ocean, the obvious test is to see whether the box diffusion model can remove to the sea an adequate amount of excess  $\text{CO}_2$ . As pointed out by Oeschger and his co-workers, their model can explain only about 80 percent of the missing  $\text{CO}_2$ . In their modeling they were forced to introduce a terrestrial biosphere growth term to make the fossil fuel  $\text{CO}_2$  budget balance. It is here that the major criticism of the Oeschger and others model comes. Baes and others (1976), Bolin (1977), Adams, Montovani, and Sundell (1977), Woodwell and Houghton (1977), Woodwell and others (1978), and Wong (1978a,b) all conclude that the terrestrial biomass has decreased over the past 20 years (*ie*, the time period covered by Keeling's measurements). If the direct estimates of the terrestrial biomass change are used to estimate the amount of fos-

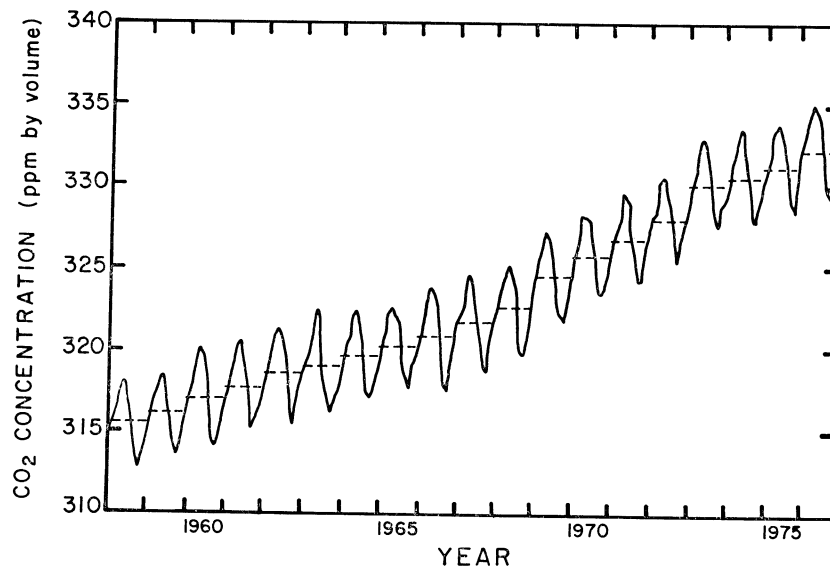


Fig 5. Measurements of the atmospheric  $\text{CO}_2$  partial pressure at Mauna Loa, Hawaii, by Keeling and Bacastow (1977). In the 16-year period between 1958 and 1974 the  $\text{pCO}_2$  rose from  $316$  to  $331 \times 10^{-9}$  atmospheres. This  $15\text{ppm}$  increase can be compared to the value of  $27\text{ppm}$  expected if all the  $\text{CO}_2$  produced by fossil fuel consumption during this period remained airborne. This yields an atmospheric fraction of  $.56$ . The uncertainty in this value is probably no larger than  $.07$  (*ie*,  $15\%$ ).

sil fuel CO<sub>2</sub> which has entered the ocean, far larger ocean inventories are obtained than given by the Oeschger and others model or, for that matter, any existing ocean model. As summarized in table 8, the differences lie well beyond any reasonable uncertainty in the parameters in the Oeschger and others calculation, either the ocean model or the biomass inventory estimates must be seriously in error. In the sections which follow, we will first give a general critique of the terrestrial biomass calculation and then make a first attempt at an "improved" ocean model. Our conclusion will be that the error lies in the biomass estimates rather than in the existing ocean models.

*Critique of attempts to reconstruct changes in terrestrial biomass  
for the last two decades*

Estimates of terrestrial biomass change are based almost entirely on the rate of forest cutting and burning. Although Bolin attempts to account for reforestation of previous agricultural land none of the estimates takes into account the rate of regrowth of previously cut forests. The importance of this is shown diagrammatically in figure 6. The large expansion of agricultural land referred to by Wilson (1978) as the "pioneer effect" was largely complete early in the present century. Since then, most of the forest cutting and burning has been on lands dedicated to forestry. As the regrowth of previously cut forests requires many decades, any adequate terrestrial biomass budget must account for this regrowth. None has. In a sense, we are concerned with the differential cutting rate rather than the absolute cutting rate. Unfortunately, we know far too little about the details of the response function shown diagrammatically in figure 6 to permit this calculation to be carried out reliably.

A further complication is that the CO<sub>2</sub> build-up in the atmosphere may have significantly increased the growth rate in forests. This in turn may also have increased the standing crop of terrestrial organic matter over that which it would have been in the absence of this excess CO<sub>2</sub>. This has been the basis for the explanation of the unaccounted for fossil

TABLE 8

Comparison of global anthropogenic CO<sub>2</sub> budgets for the period 1955 to 1973 inferred from ocean modeling and from forest assays. In the ocean model inventories the change in terrestrial biomass is obtained by difference. In the forest biomass assays the ocean uptake of CO<sub>2</sub> is obtained by difference. The values in the table are given in units of  $0.46 \times 10^{14}$  moles of carbon.

	Woodwell	Bolin	Geochemical models
Fossil fuel CO <sub>2</sub> produced	100	100	100
Release of CO <sub>2</sub> from terrestrial biomass reduction	100	20	-10*
Total input of anthropogenic CO <sub>2</sub>	200	120	90
Observed atm increase	55	55	55
Ocean uptake	145*	65*	35

\* Calculated by difference.



fuel CO<sub>2</sub> in geochemical models. Unfortunately, there is, as yet, no way to quantify this effect. Like regrowth in previously cut forests, it will reduce the estimates of inventory change based on cutting and burning.

Stuiver (1978), Freyer (1979), and Freyer (in press) have pointed out that the change in the <sup>13</sup>C/<sup>12</sup>C ratio as recorded by tree rings might be used to determine the sum of the contributions of fossil fuel CO<sub>2</sub> and terrestrial biomass CO<sub>2</sub>. Keeling, Bacastow, and Tans (in press) have pointed out, however, that when the possibility that an isotope separation of magnitude similar to that for photosynthesis occurs when CO<sub>2</sub> invades the sea is considered, this approach becomes ambiguous. Also, because the noise in tree ring <sup>13</sup>C/<sup>12</sup>C data due to factors other than the change in the <sup>13</sup>C/<sup>12</sup>C ratio in atmospheric CO<sub>2</sub> appears to be as large as the signal of interest, more work has to be done before the tree-ring record can be accepted as a valid proxy for the atmospheric record.

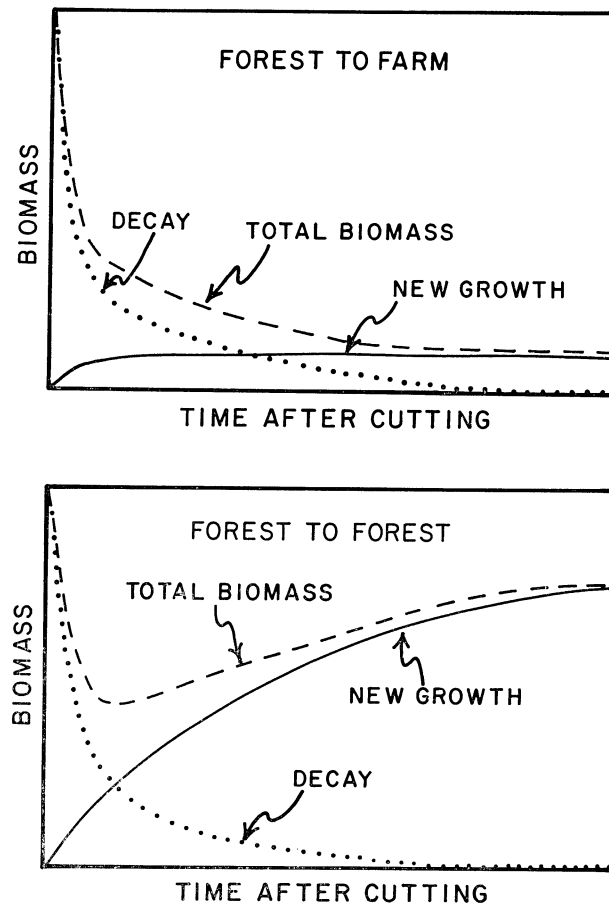


Fig 6. Hypothetical curves for biomass as a function of time after forest cutting.

Thus, at this point, we can only say that the potential for significant  $\text{CO}_2$  transfer between the atmosphere and terrestrial biosphere is certainly large enough that it must be accepted as a significant term in any carbon budget. However, in our estimation it is not possible to say whether the change over the last two decades has been positive or negative. Thus, the terrestrial biomass data can be used neither to support nor to cast doubt on the ocean models.

*Toward an improved ocean model*

Anyone familiar with the water mass structure and ventilation dynamics of the ocean will quickly realize that the box-diffusion model is by no means a realistic representation. No simple modification to the model will substantially improve the situation. To do so we must take a giant step in complexity to a new generation of models that attempt to account for the actual geometry of ventilation of the sea. We are as yet not in a position to do this in a serious way. At least a decade will pass before a realistic ocean model can be developed.

As an interim strategy we propose to concentrate on a model which emphasizes those processes in the ocean that operate on time scales up to about 30 years. The reason for this choice is that the mean age of fossil fuel  $\text{CO}_2$  molecules is now about 30 years and will remain close to this value as long as our fossil fuel use rises at the rate of several percent per year (see fig 7). Thus, for predictions of atmospheric  $\text{CO}_2$  content over the interval during which we are heavily dependent on fossil fuels (*ie*, the next 50 to 90 years) there is no need to consider processes in the ocean which operate time scales much larger than 30 years. Only a very small fraction of the fossil fuel  $\text{CO}_2$  molecules will by chance become involved in these long-time scale processes.

On the time scale of 30 years the processes to be considered are the ventilation of the main thermocline, the formation of new deep water,

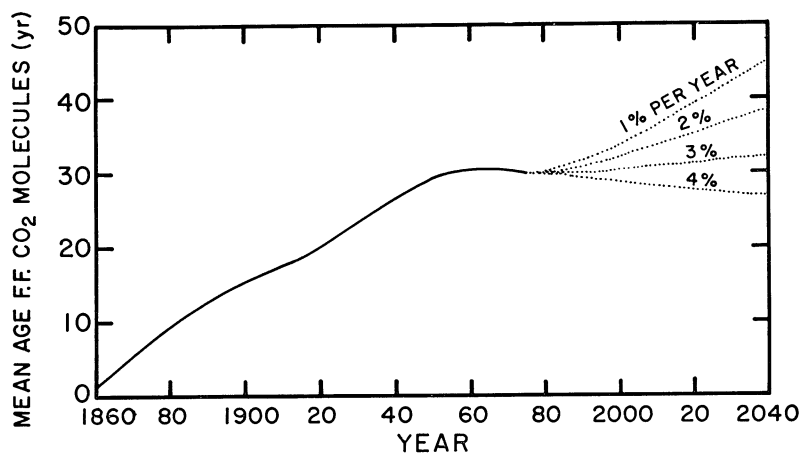


Fig 7. Mean age of fossil fuel  $\text{CO}_2$  molecules as function of time. Future mean ages for various fossil fuel use scenarios are also given (dotted lines).

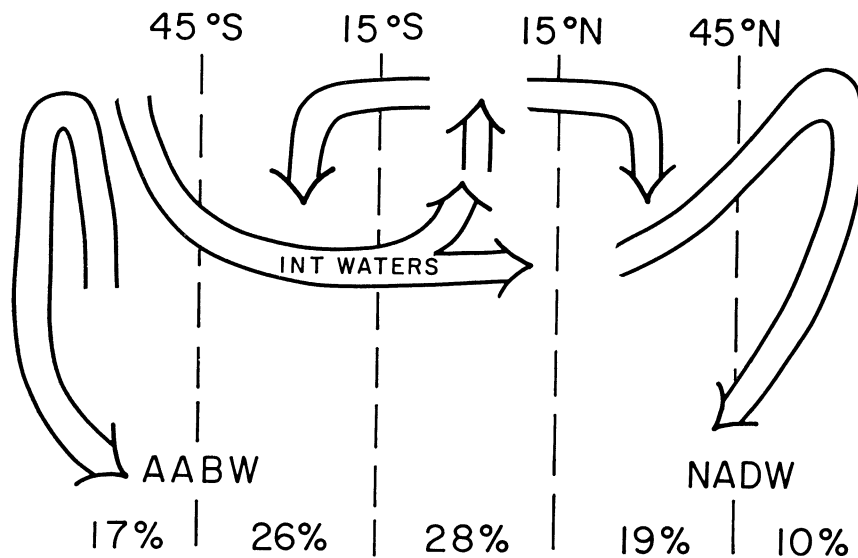


Fig 8. Diagram shows the patterns of the flow within the ocean. Upwelling occurs in the equatorial zone, downwelling occurs in the temperate zone and polar zone. The ocean area in each zone is shown as percentage of total ocean area.

and the ventilation of the intermediate water masses. As on this time scale the deep sea acts as an infinite reservoir, the details of its ventilation pathways need not be known. Also, the rate at which fossil fuel  $\text{CO}_2$  interacts with the  $\text{CaCO}_3$  in deep sea sediments need not be considered. The approximate time scales for various oceanic processes are summarized in table 9.

The processes needing consideration are shown diagrammatically in figure 8. For the purposes of modeling, we have divided the waters of the oceans into three major categories: equatorial ( $<15^\circ$ ), temperate ( $15^\circ\text{-}45^\circ$ ), and polar ( $>45^\circ$ ). The logic behind this division will become apparent in the sections which follow.

TABLE 9  
Ocean processes to be considered  
on various time scales

3-30 years
Main thermocline ventilation
Formation of new deep water
10-100 years
Intermediate water ventilation
100-1000 years
Ventilation of the deep sea
1000-10,000 years
Calcite dissolution in the deep sea

A further aspect of our strategy is to develop an analogue model designed to match the distribution of the bomb-produced tracers. As of the time of the GEOSECS survey, these isotopes had had, on the average, 10 years to penetrate into the sea (see fig 9). As of 1980, they will have had, on the average, 17 years to penetrate the system. Thus, any model that properly distributes the bomb-produced tracers  $^{14}\text{C}$ ,  $^3\text{H}$ ,  $^3\text{He}$ ,  $^{85}\text{Kr}$  . . . which are readily measured in the sea should adequately distribute fossil fuel  $\text{CO}_2$  currently not measurable in the sea. As time passes, the characteristic times for the bomb tracers and for fossil fuel  $\text{CO}_2$  will become more nearly equal.

#### *Equatorial and temperate thermocline*

Taken together, the equatorial and temperate zones cover 73 percent of the ocean area. Penetration of waters from the surface into the thermoclines underlying this area constitutes, in our estimation, the most important short term (*ie*, 30-year time scale) sink for fossil fuel  $\text{CO}_2$ .

Broecker, Peng, and Stuiver (1978) indicated that the oceanic penetration of the bomb-produced tracers is quite different in the equatorial than in the temperate zones of the Atlantic and Pacific Oceans. The excess  $\Delta^{14}\text{C}$  over the pre-nuclear value is greater in the temperate zone than in the equatorial zone (fig 10). The penetration depth of excess  $^{14}\text{C}$  is much greater in the temperate zone than in the equatorial zone (fig 11). These two observations lead to higher water column inventories of bomb  $^{14}\text{C}$  in the temperate than in the equatorial zone (fig 12).

These observations are consistent with the view of most oceanographers that upwelling of intermediate depth water occurs in the equatorial zone. Such upwelling is expected from the divergence of the surface currents driven by the trade winds (fig 13). It expresses itself by a shoaling of the isopycnal surfaces under the equatorial zone (fig 14) and by high  $\text{CO}_2$  partial pressures in equatorial surface waters (fig 15).

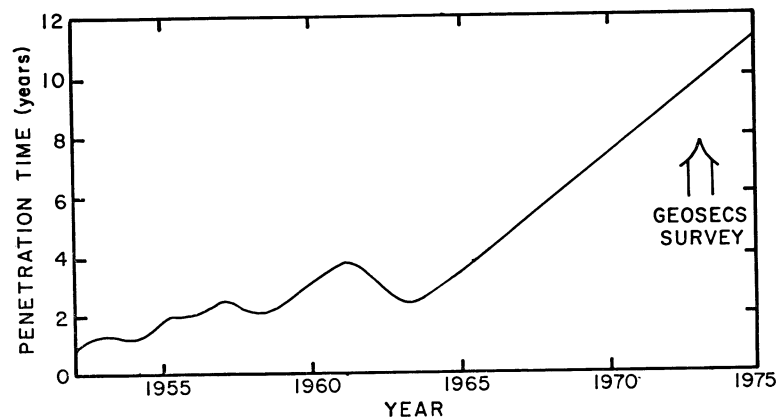


Fig 9. The mean penetration time for the bomb produced tritium present in the ocean as a function of time.

We have made a simple mixing model that is consistent with these observations. It involves upwelling of water that, as of 1973, was not yet contaminated with bomb products. Upon reaching the surface, this upwelled water flows poleward, along the surface, and downwells in the adjacent temperate zones. Superimposed on the upwelling in the equatorial zone and the downwelling in the temperate zone is vertical eddy mixing. The absolute rate of these processes is fixed from our independent knowledge of the rate of  $\text{CO}_2$  invasion. That this model adequately explains the distribution of bomb produced  $^{14}\text{C}$  in the equatorial and north temperate Atlantic is seen in figure 16, where the model profile and mean observed profiles, for 1972-1973, are compared, and in figure 17, where the time trend in north temperate Atlantic surface water is contrasted with the measurements made by Druffel and Linick (1978) on

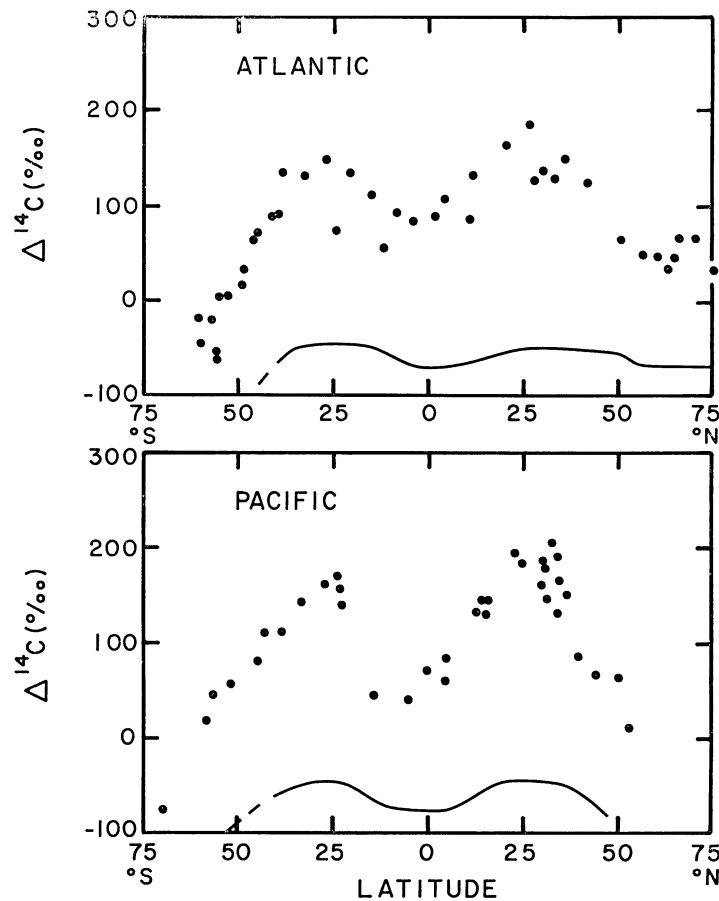


Fig 10. Surface water  $\Delta^{14}\text{C}$  value as function of latitude in the Pacific and Atlantic Oceans. The measurements were made by Stuiver, University of Washington, and Östlund, University of Miami, on samples collected as part of the GEOSECS program (1972-1974). The prebomb  $\Delta^{14}\text{C}$  trend is given by the solid lines.

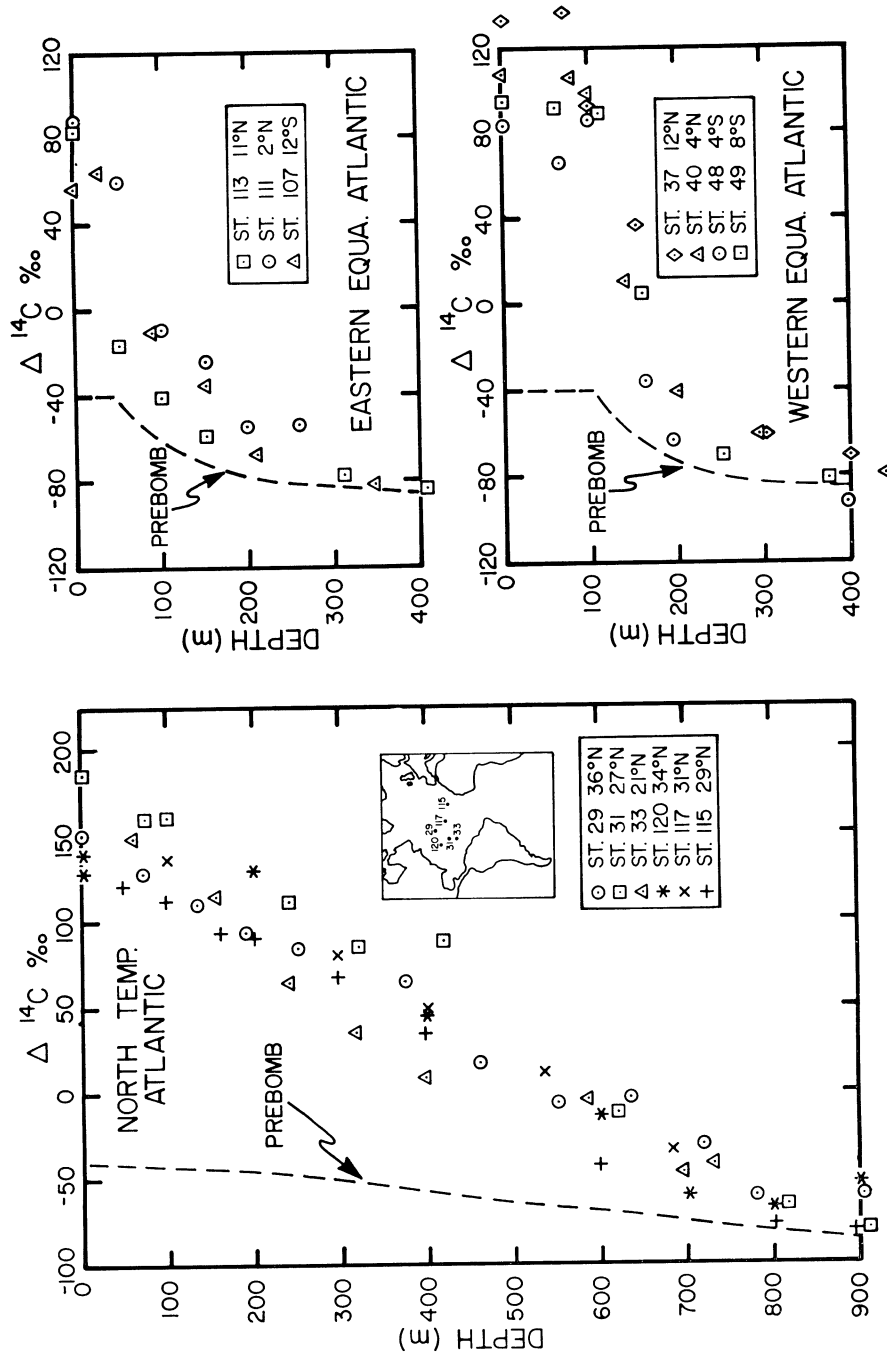


Fig. 11. Penetration of bomb produced  $^{14}\text{C}$  into the north temperate Atlantic and into the equatorial Atlantic as measured during the GESECS program by Stuiver and Östlund.

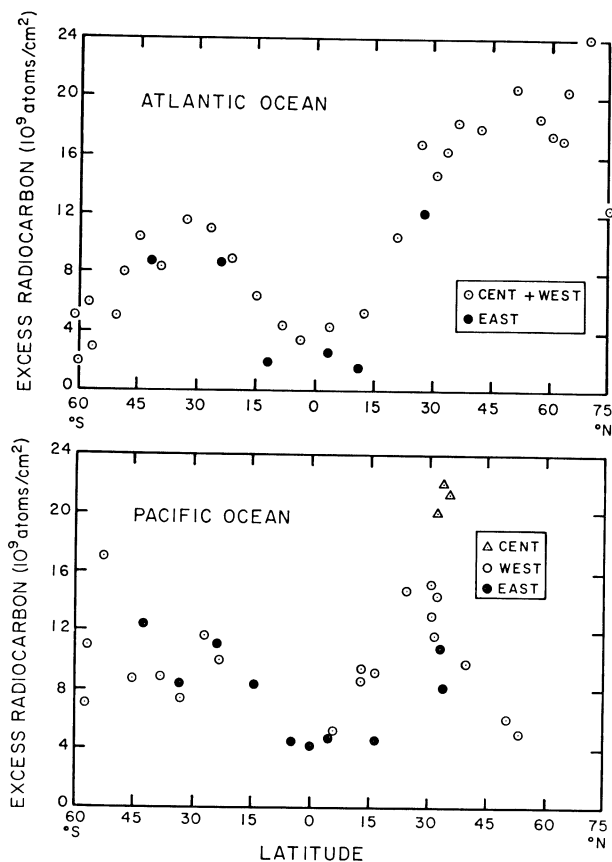


Fig 12. Water column inventories ( $10^9$  atoms/cm<sup>2</sup>) of bomb produced <sup>14</sup>C at various of the GEOSECS stations in the Atlantic (upper panel) and Pacific (lower panel). The measurements upon which these inventories are based were made by Stuiver and Östlund.

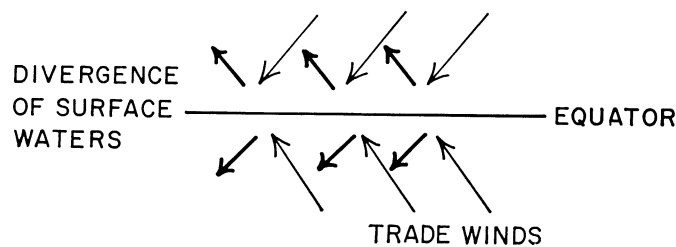


Fig 13. Trade winds converging from the northeast and southeast toward the equator drive the surface waters toward the northwest and southwest causing a divergence of water at the equator. This water is replaced from below through upwelling.

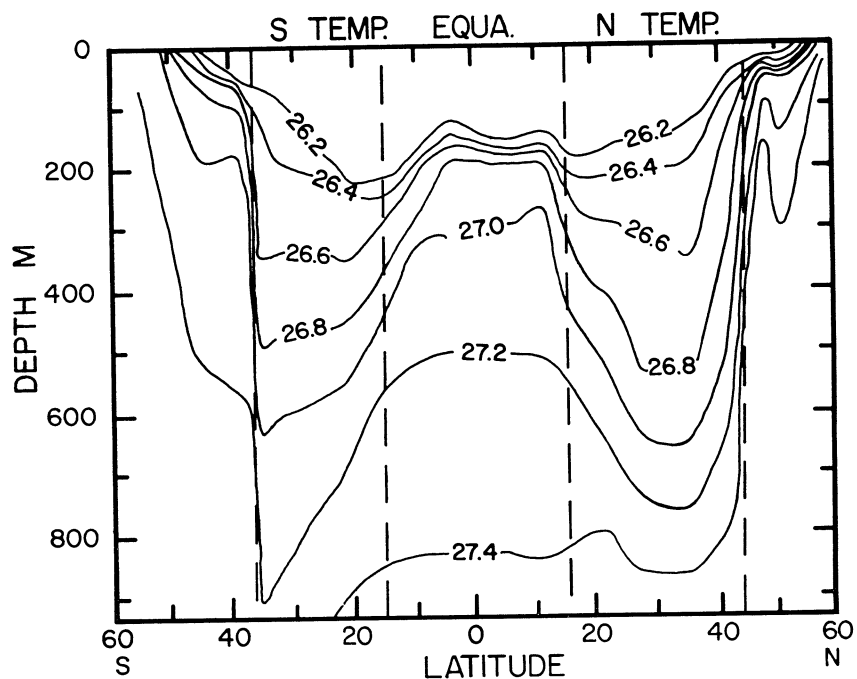


Fig 14. Depth of various isopycnal horizons (surfaces along which potential density remains constant) along the GEOSECS track in the western Atlantic.

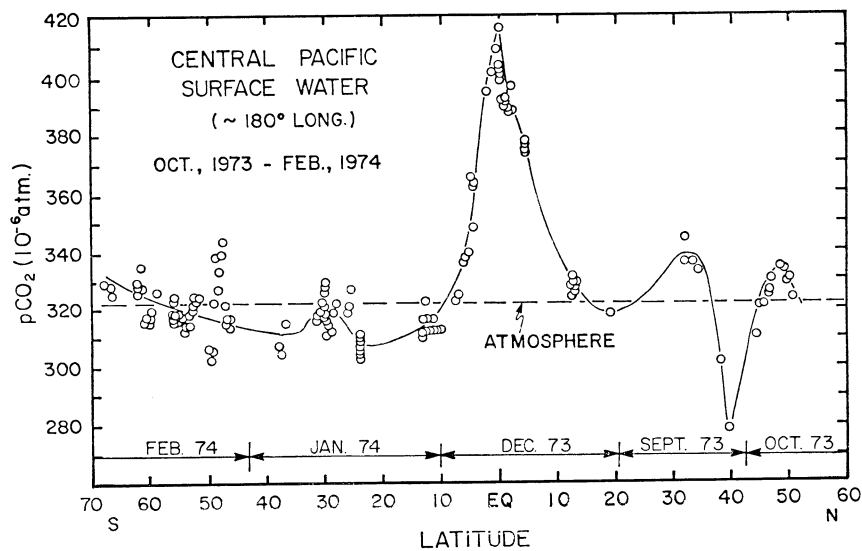


Fig 15. Partial pressure of carbon dioxide in surface water along the GEOSECS track in the central Pacific ( $180^\circ$  longitude) as measured by Takahashi of the Lamont-Doherty Geological Observatory.



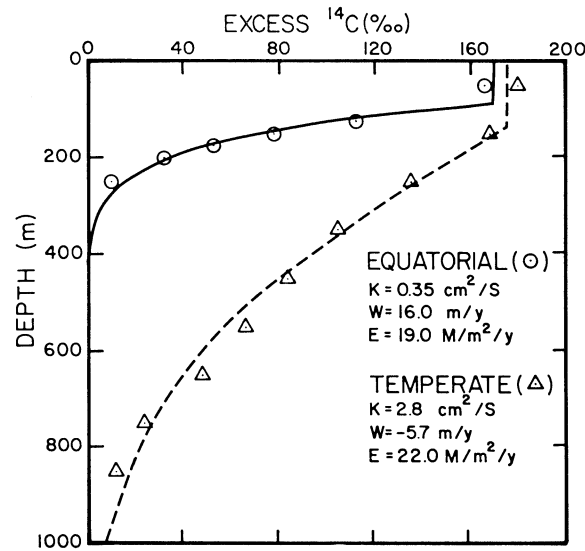


Fig 16. Comparison of the model produced profiles of excess bomb-produced  $^{14}\text{C}$  in the equatorial and north temperate zone with the average observations (from fig 11). The parameter values ( $\text{CO}_2$  invasion rates, upwelling rate, and vertical diffusivity) are given on the diagram.

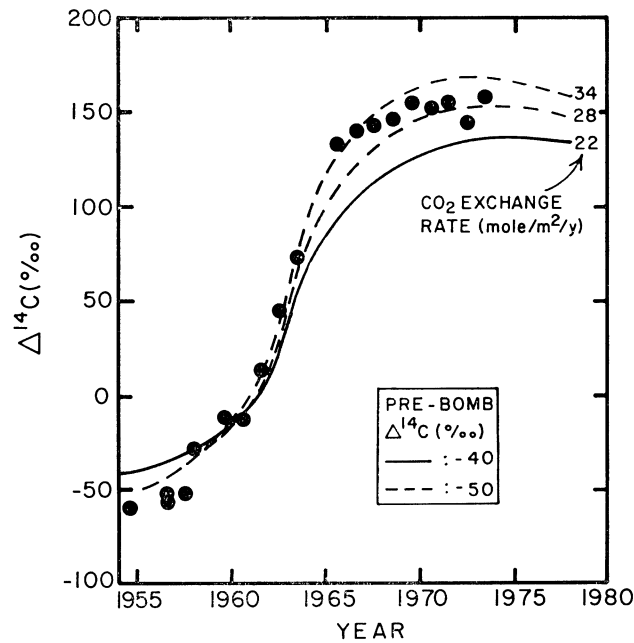


Fig 17. Comparison of the time trend of  $\Delta^{14}\text{C}/\text{‰}$  in a growth ring dated coral (as measured by Druffel and Linick, 1978) from the Florida Straits with the prediction (solid line) based on our model for the north temperate Atlantic. A better fit curve (dashed) would require an exchange rate of about  $28 \text{ moles/m}^2/\text{yr}$  and a pre-bomb surface  $\Delta^{14}\text{C}$  of  $-50\text{‰}$ .

a ring-dated coral from the Florida Straits. Further support of the model comes from its ability to generate the observed profiles of  $^3\text{H}$  and  $^3\text{He}$  in the north temperate and equatorial Atlantic (fig 18) and the time trend of tritium observed for the north temperate Atlantic (fig 19). The modeling was done using the tritium delivery function to the surface Atlantic ocean suggested by Weiss, Roether, and Dreisigacker (1978).

#### Polar Ocean

Three processes must be considered in the polar oceans: the penetration of fossil fuel  $\text{CO}_2$  into the polar thermocline, the formation of intermediate water, and the formation of deep water. All three are likely to be significant in the current uptake of fossil fuel  $\text{CO}_2$  by the ocean. For the purposes of this discussion, the polar sea will be subdivided into three parts: the northern Atlantic, including the Arctic, the northern Pacific, including the Bering Sea, and the Antarctic. Intermediate waters form in all three regions, and deep waters in just two, the Antarctic and northern Atlantic. The Antarctic constitutes 17 percent of the ocean area, while the high latitude North Atlantic and Pacific constitute 10 percent.

The process of intermediate water formation is not well understood. We have only limited bomb tracer data for these water masses. For this analyses we exclude their role in removing fossil fuel  $\text{CO}_2$  from the air. The error in the overall total sustained by this omission is probably not large.

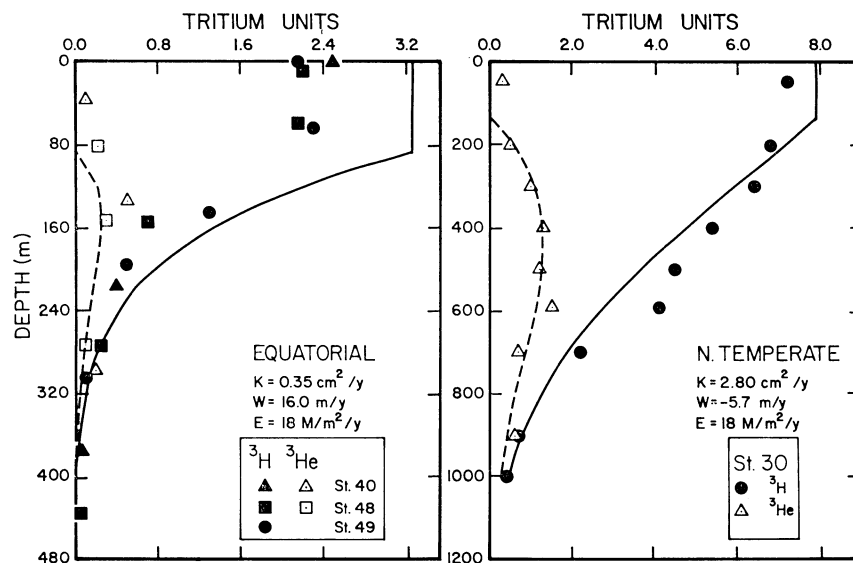


Fig 18. Comparison between the model generated (1973) and observed (GEOSECS) profiles of tritium and its daughter product  $^3\text{He}$  for the equatorial and north temperate regions of the ocean. The observations are for GEOSECS Stations 40, 48, and 49 in the equatorial zone and for GEOSECS Station 30 in the north temperate zone. The data was obtained by Jenkins and Clark (1976) at McMaster University in Canada.

In order to assess the importance of deep water formation in the removal of fossil fuel  $\text{CO}_2$  from the atmosphere, we need to know the flux of waters to the deep sea from the source regions and the extent to which these waters reach equilibrium with the atmosphere prior to their descent to the abyss. In the calculations below, we will use a flux of 30 Sverdrups for deep water formation in the North Atlantic (Broecker, 1979) and of 40 Sverdrups (Gill, 1973; Gordon, 1975; Killworth, 1974; 1977; Carmack, 1977) for the deep water formation in the Antarctic. Both figures lie at the high end of the range of literature values.

The degree to which these waters achieve  $\text{CO}_2$  equilibrium with the atmosphere is not known. Table 10 shows that the time required for a surface water mixed layer to chemically equilibrate with the atmosphere is on the order of one year. In both the Antarctic and northern Atlantic the source for deep water is *not* water from the adjacent surface ocean but rather intermediate or deep water. These waters presumably enter the source zone largely free of fossil fuel  $\text{CO}_2$  and must gain it during their residence in the source region (fig 8). Because of its long equilibration time,  $^{14}\text{CO}_2$  is not the ideal analogue for  $\text{CO}_2$  (table 10). However, the fact that there is little evidence for  $^{14}\text{CO}_2$  uptake from the air by newly formed Antarctic Bottom Water (Wiess, Ostlund, and Craig, 1979) suggests that  $\text{CO}_2$  equilibration is far from complete for these waters. Waters descending in the northern Atlantic are also deficient in  $^{14}\text{CO}_2$  ( $\Delta^{14}\text{C} \cong -70\text{‰}$ ). As it is not possible to say what  $\Delta^{14}\text{C}$  value they had upon entering the source region, it is not possible to say to what extent equilibration occurred. In the calculations below, we use guesses of 25 percent the equilibrium fossil fuel  $\text{CO}_2$  content for deep waters forming in the Antarctic and 75 percent the equilibrium fossil fuel  $\text{CO}_2$

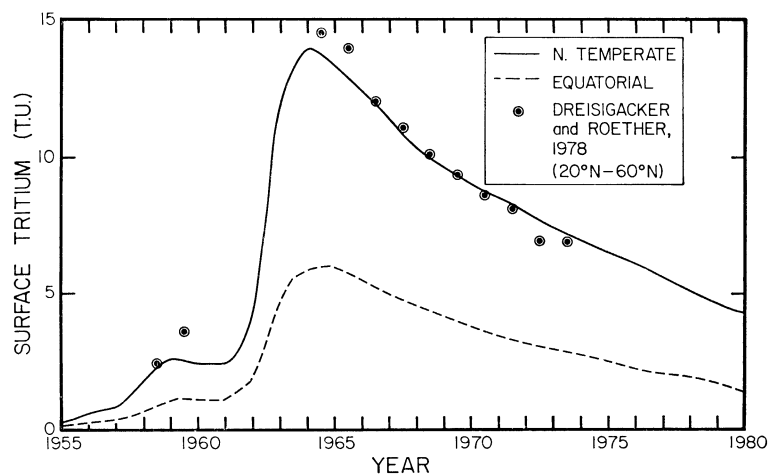


Fig 19. Comparison of the time trend of tritium observed for the surface north Atlantic (Dreisigacker and Roether, 1978) with that predicted by the model given here for the north temperate zone of the Atlantic.

content for those forming in the northern Atlantic. Only when both  $^{85}\text{Kr}$  and bomb  $^{14}\text{CO}_2$  data are available for recently formed deep waters will it be possible to improve the estimates of the degree of equilibration (Broecker, Peng, and Takahashi, in press).

Figure 20 shows that the penetration of bomb produced isotopes in the high latitude regions varies considerably from region to region and even from station to station. As we have not yet given serious attention to these areas, we are forced to make very rough approximations of their fossil fuel  $\text{CO}_2$  uptake. This is done by adopting a vertical diffusion coefficient of  $3.0\text{cm}^2/\text{sec}$  for the entire region.

*Preliminary estimate of fossil fuel  $\text{CO}_2$  uptake by regional model*

Based on the above assumptions for the equatorial, temperate, and polar oceans, we have attempted to determine whether use of a regional ocean model significantly alters the amount of fossil fuel  $\text{CO}_2$  taken up by the ocean (over that obtained using the box-diffusion model). In this endeavor we avoid the need for a biospheric model by using what we refer to as a model intercomparison atmospheric  $\text{CO}_2$  history. This input function (fig 21) is a reconstruction of the atmospheric  $\text{CO}_2$  content over the last 100 years. It is based on the observations of Keeling and Bacastow (1977) back to 1958. Prior to this, the assumption is made that the atmospheric increase during any given year was half the  $\text{CO}_2$  production during that year. While this function cannot be used to determine the absolute uptake of  $\text{CO}_2$  by the ocean, it can be used to determine the relative uptakes achieved by different models.

Using this input function we calculate the ocean uptake by the Oeschger and others model and by our regionalized analogue model. Table 11 summarizes the assumptions used. The resulting fossil fuel  $\text{CO}_2$  uptakes, as of 1973, are also given in this table. The depth distribution of excess fossil fuel  $\text{CO}_2$ , in 1973, for the temperate and equatorial zones are compared to that for the Oeschger and others ocean in figure 22. The

TABLE 10  
Equilibration times between the surface ocean mixed layer  
and the atmosphere for various gases

$\text{Kr}^{85}$	$\tau = \frac{h}{v} \cong 30 \text{ days}$
$\text{CO}_2$ (chemical)	$\tau = \frac{h}{v} \frac{[\Sigma\text{CO}_2]}{[\text{CO}_2]} \frac{1}{R} = 350 \text{ days}$
$^{14}\text{CO}_2$ (isotopic)	$\tau = \frac{h}{v} \frac{[\Sigma\text{CO}_2]}{[\text{CO}_2]} = 4500 \text{ days}$

where

$h$  = mixed layer thickness  $\cong 75\text{m}$   
 $v$  = piston velocity  $\cong 2.5\text{m/day}$

$$\frac{[\Sigma\text{CO}_2]}{[\text{CO}_2]} \cong \frac{2100}{14} \cong 150$$

$R$  = Revelle factor  $\cong 13$

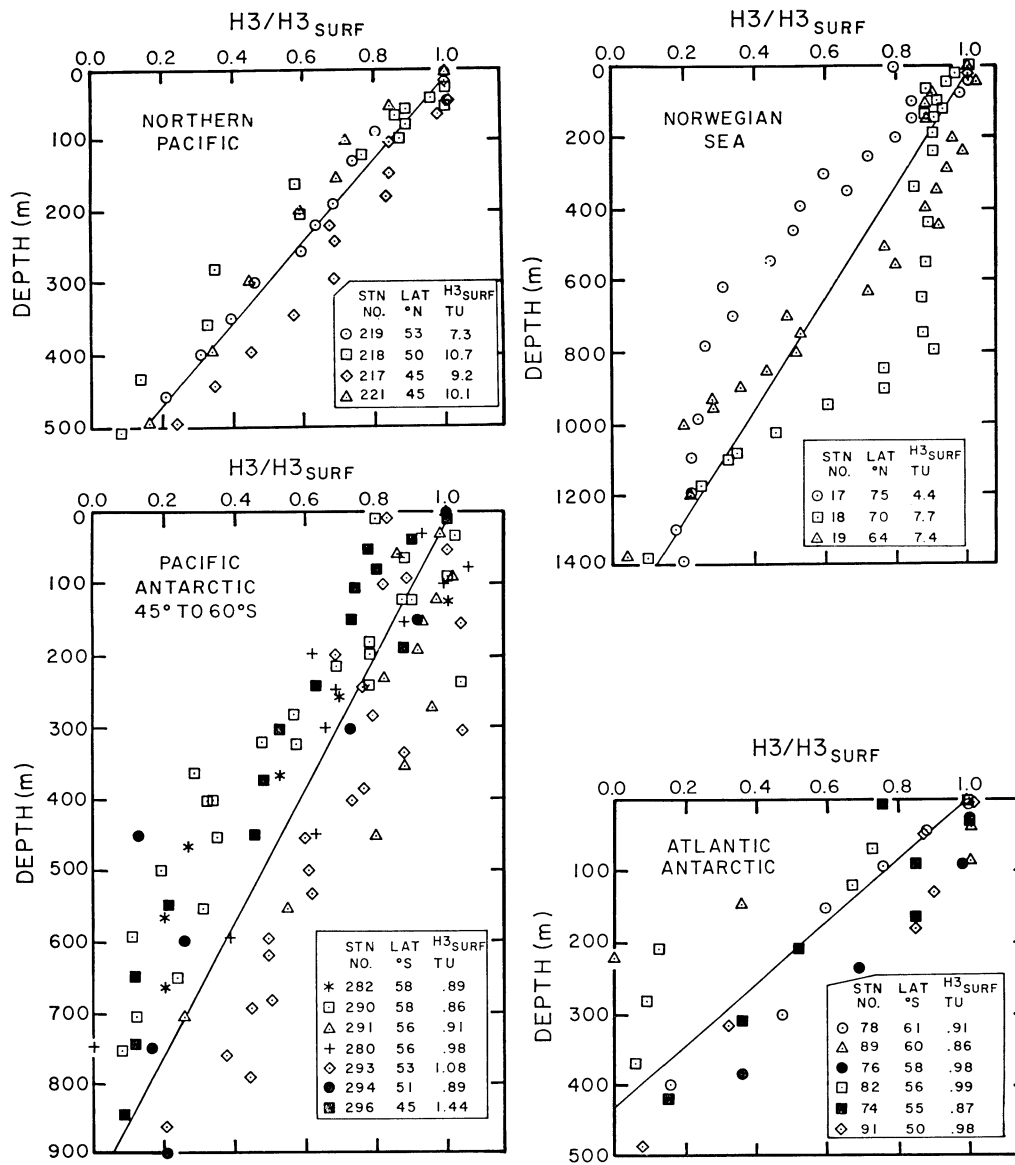


Fig 20. Composite profiles of tritium in the polar regions as measured by the GEOSECS groups. The tritium is expressed relative to the concentration in surface water.



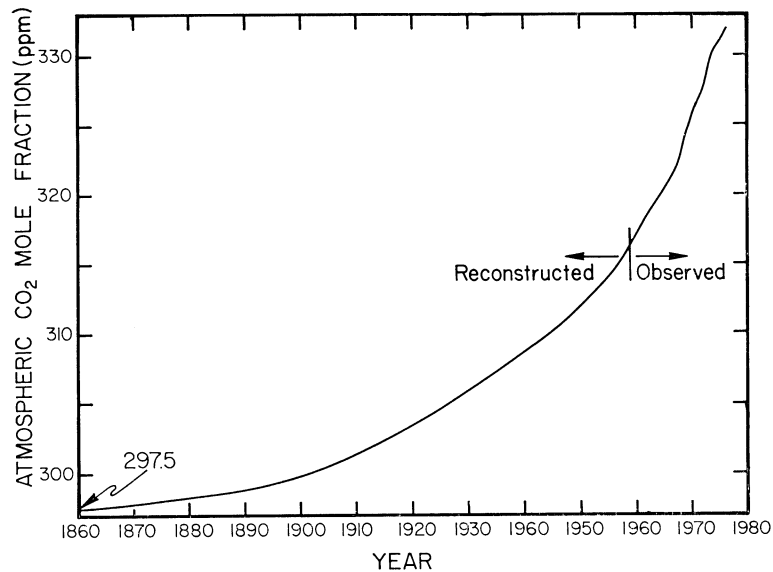


Fig 21. The model comparison atmospheric CO<sub>2</sub> history reconstructed assuming that prior to the onset of the measurements by Keeling and his co-workers in 1958 the rise in atmospheric CO<sub>2</sub> content each year was half the amount added by fossil fuel CO<sub>2</sub> burning.

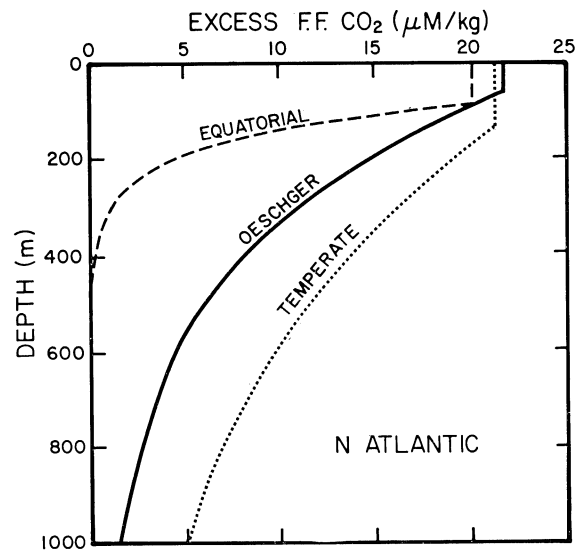


Fig 22. Comparison of the depth distributions for the temperate and equatorial zones of the regional model with that for the Oeschger and others box-diffusion model.

result is that the uptake by our regional ocean model is  $44 \times 10^{14}$  moles, while that for the box-diffusion model as calibrated by Oeschger and others is  $29 \times 10^{14}$  moles and as calibrated here is  $35 \times 10^{14}$  moles (table 7).

#### CONCLUSION

Based on this analysis, we conclude that the box-diffusion model gives an excellent representation of atmosphere-ocean  $\text{CO}_2$  and  $^{14}\text{CO}_2$  interactions on time scales up to several tens of years. It very likely gives adequate short-term predictions of the increase in atmospheric  $\text{CO}_2$  to be expected for any given fossil fuel  $\text{CO}_2$  use scenarios. When coupled with an adequate model for the replacement of living terrestrial biospheric and soil carbon with atmospheric carbon, it will also provide the best current means of deconvolving the  $^{14}\text{C}$  production rate changes needed to account for the temporal changes in  $^{14}\text{C}/\text{C}$  ratio observed in the tree-ring record (Stuiver and Quay, 1980). We suggest, however, that a somewhat higher diffusivity (2.2 rather than  $1.25\text{cm}^2/\text{sec}$ ) be used in this model.

#### ACKNOWLEDGMENTS

This paper depends heavily on results obtained as part of the GEOSECS program. The success of this global survey is a tribute to the efforts of the late Arnold Bainbridge. He directed the development and the operation of the shipboard systems. His ability to orchestrate this enormous undertaking so effectively was truly amazing.

Financial support for this work was provided by a grant from the International Decade for Ocean Exploration Program of the National Science Foundation (OCE 78-09857). Lamont-Doherty Geological Observatory contribution no. 2978.

#### REFERENCES

- Adams, J A S, Montovani, M S M, and Sundell, L L, 1977, Wood versus fossil fuel as a source of excess carbon dioxide in the atmosphere: a preliminary report: *Science*, v 196, p 54-56.
- Baes, C F, Goeller, H E, Olsen, J S, and Rotty, R M, 1976, The global carbon dioxide problem: Oak Ridge Natl Lab ORNL 5191, p 1-78.
- Bolin, B, 1977, Changes of land biota and their importance for the carbon cycle: *Science*, v 196, p 613-615.
- Broecker, W S, 1979, A revised estimate for the radiocarbon age of North Atlantic Deep Water: *Jour Geophys Research*, v 84, p 3218-3226.
- Broecker, W S, Peng, T-H, and Stuiver, Minze, 1978, An estimate of the upwelling rate in the equatorial Atlantic based on the distribution of bomb radiocarbon: *Jour Geophys Research*, v 83, p 6179-6186.
- Broecker, W S, Peng, T-H, and Takahashi, T, in press, A strategy for the use of bomb-produced radiocarbon as a tracer for the transport of fossil fuel  $\text{CO}_2$  into the deep sea source regions: *Earth Planetary Sci Letters*, in press.
- Broecker, W S, Takahashi, T, Simpson, H J, and Peng, T-H, 1979, Fate of fossil fuel carbon dioxide and the global carbon budget: *Science*, v 206, p 409-418.
- in press, The fate of fossil fuel  $\text{CO}_2$ : Can the global carbon budget be balanced?: *Science*, in press.
- Carmack, E C, 1977, Water characteristics of the Southern Ocean south of the Polar Front, in Angel, M, ed, *A voyage of discovery*: New York, Pergamon Press, p 15-44.
- Craig, Harmon, 1957, The natural distribution of radiocarbon and the exchange time of carbon dioxide between atmosphere and sea: *Tellus*, v 9, p 1-17.



- Dreisigacker, E and Roether, Wolfgang, 1978, Tritium and  $^{90}\text{Sr}$  in North Atlantic surface water: *Earth Planetary Sci Letters*, v 38, p 301-312.
- Druffel, E M, 1980, Radiocarbon in annual coral rings of Belize and Florida, *in* Stuiver, Minze, and Kra, Renee, eds, Internatl radiocarbon conf, 10th, Proc: Radiocarbon, v 22, no. 2, p 363-371.
- Druffel, E M and Linick, T W, 1978, Radiocarbon in annual coral rings in Florida: *Geophys Research Letters*, v 5, p 913-916.
- Freyer, H D, 1979, Estimate of the past biospheric  $\text{CO}_2$  uptake into the atmosphere from  $^{13}\text{C}$  tree-ring data: *EOS (Am Geophys Union Trans)* v 60, p 266.
- in press, On the  $^{13}\text{C}$  record in tree rings  $^{13}\text{C}$  variations in northern hemispheric trees during  $\text{CO}_2$  increase: *Tellus*, in press.
- Garrett, C, 1979, Mixing in the ocean interior: *Dynamics of Atmospheres and Oceans*, v 3, p 239-265.
- Gill, A E, 1973, Circulation and bottom water production in the Weddell Sea: *Deep Sea Research*, v 20, p 111-140.
- Gordon, A L, 1975, General ocean circulation, *in* Reid, R O, ed, Numerical models of ocean circulation: Washington, DC, Natl Acad Sci, p 39-53.
- Jenkins, W J and Clark, W B, 1976, The distribution of  $^3\text{He}$  in the western Atlantic Ocean: *Deep Sea Research*, v 23, p 481.
- Keeling, C D and Bacastow, R C, 1977, Impact of industrial gases on climate, *in* Energy and climate: Washington, DC, Natl Acad Sci, p 72-95.
- Keeling, C D, Bacastow, R C, and Tans, P P, in press, Predicted shift in the  $^{13}\text{C}/^{12}\text{C}$  ratio of atmospheric carbon dioxide: *Geophys Research Letters*, in press.
- Killworth, P D, 1974, A baroclinic model of motions on Antarctic continental shelves: *Deep Sea Research*, v 21, p 815-837.
- 1977, Mixing on the Weddell Sea continental slope: *Deep Sea Research*, v 24, p 427-448.
- Machta, L, 1972, The role of the oceans and the biosphere in the  $\text{CO}_2$  cycle, *in* Dryssen, D, ed, Changing chemistry of the oceans, Nobel Symposium No. 20, Stockholm.
- Nozaki, Y, Rye, D M, Turekian, K K, and Dodge, R E, 1978, A 200-year record of carbon-13 and carbon-14 variations in a Bermuda coral: *Geophys Research Letters*, v 5, p 825-828.
- Nydal, Reidar, Lövseth, Knut, and Gulliksen, Steiner, 1979, A survey of radiocarbon variation in nature since the Test Ban Treaty, *in* Berger, Rainer and Suess, H E, eds, Radiocarbon dating, Internatl radiocarbon conf, 9th, Proc: Berkeley/Los Angeles, Univ California Press, p 313-323.
- Oeschger, Hans, Siegenthaler, Ulrich, Schotterer, Ulrich, and Gugelmann, A, 1975, A box diffusion model to study the carbon dioxide exchange in nature: *Tellus*, v 27, p 168-192.
- Ostlund, H G, Brescher, R, Olsen, R, and Ferguson, M J, 1978, Tritium laboratory report #8, GEOSECS Pacific radiocarbon and tritium results: Univ Miami, RSMAS, Miami, Florida.
- Ostlund, H G, Dorsey, H G, and Brescher, R, 1976, Tritium laboratory data report #5, GEOSECS Atlantic radiocarbon and tritium results: Univ Miami, RSMAS, Miami, Florida.
- Peng, T-H, Broecker, W S, Mathieu, G G, and Li, Y-H, 1979, Radon evasion rates in the Atlantic and Pacific Oceans as determined during the GEOSECS program: *Jour Geophys Research*, v 84, p 2471-2486.
- Schlesinger, W H, 1977, Carbon balance in terrestrial detritus: *Ann Rev Ecol Systems*, v 8, p 51-81.
- SIPRI Yearbook 1975, 1976, World armament and disarmaments: Stockholm, Almqvist & Wiksell.
- Stuiver, Minze, 1978, Atmospheric carbon dioxide and carbon reservoir changes: *Science*, v 199, p 253-258.
- Stuiver, Minze and Quay, P D, 1980, Patterns of atmospheric  $^{14}\text{C}$ , *in* Stuiver, Minze and Kra, Renee, eds, Internatl radiocarbon conf, 10th, Proc: Radiocarbon, v 22, no. 2, p 166-176.
- Suess, H E, 1955, Radiocarbon concentration in modern wood: *Science*, v 122, p 415-417.
- Weiss, R F, Ostlund, H G, and Craig, Harmon, 1979, Geochemical studies of the Weddell Sea: *Deep-Sea Research*, v 26, p 1093-1120.
- Weiss, Wolfgang, Roether, Wolfgang, and Dreisigacker, E, 1978, Tritium in the North Atlantic Ocean: inventory, delivery, and transfer into the deep water, *in* Internatl symposium on the behaviour of tritium in the environment: San Francisco, IAEA-SM-232/98.

- Whittaker, R L and Likens, G E, 1975, The biosphere and man, *in* Lieth, H and Whittaker, R L, eds, Primary productivity of the biosphere, Ecol Study 14: New York, Springer-Verlag, p 305-328.
- Wilson, A T, 1978, Pioneer agriculture explosion and CO<sub>2</sub> levels in the atmosphere: *Nature*, v 273, p 40-41.
- Wong, C S, 1978a, Atmospheric input of carbon dioxide from burning wood: *Science*, v 200, p 197-200.
- 1978b, Carbon dioxide — a global environmental problem into the future: *Marine Pollution Bull*, v 9, p 257-264.
- Woodwell, G M and Houghton, R A, 1977, Biotic influences on the world carbon budget, *in* Stumm, W, ed, Global chemical cycles and their alterations by man: Berlin, Dahlem Konferenzen, p 61-72.
- Woodwell, G M, Whittaker, R H, Reiners, W A, Likens, G E, Delwiche, C C, and Bodkin, D B, 1978, The biota and the world carbon budget: *Science*, v 199, p 141-146.
- Zander, I and Araskog, R, 1973, Nuclear explosions 1945-1972, basic data: Försvarets Forskningsanstalt, Avd 4 Stockholm, FOA 4, rept 4505-A1, 56 p.